

GPS Positioning in the Fast Track: Track Model Constraint Enhancement for OEM4

Tom Ford, *NovAtel Inc.*

Ken Milnes, *Sportvision Inc.*

Matt Lazar, *Sportvision Inc.*

BIOGRAPHIES

Tom Ford is a GPS specialist at NovAtel Inc.. He has a BMath degree from the University of Waterloo (1975) and a BSc in survey science from the University of Toronto (1981). He did research in the inertial and GPS field at Sheltech and Nortech surveys before becoming a member of the original group of GPS developers for NovAtel Communications (now NovAtel Inc.). He has helped develop many of the core tracking and positioning technologies at NovAtel Inc. Over the past few years his focus has been to develop and implement inertial/GPS algorithms for an integrated INS/GPS system. In addition he has been developing specific GPS only positioning algorithms such as the one described in this paper.

Ken Milnes is a senior scientist and project manager at Sportvision, Inc. As a co-founder of Etak Inc., he performed extensive work in dead reckoning and digital map matching algorithms for land navigation. At SRI International, he did research on HF radar systems. He received a BS in Electrical Engineering and Computer Science from University of California at Berkeley.

Matt Lazar is an engineer at Sportvision, Inc. He received a B.S. degree in Mathematical Sciences from Stanford University, and a Ph.D. degree in Mathematics from University of California at Santa Barbara.

ABSTRACT

Sports entertainment requires that instantaneous and continuous measures of the performance of the participants are available to the television audience. In an auto racing environment this includes the relative positions, velocity and diagnostics for the vehicles in the race. Some of the information can be alphanumeric, but a graphical representation gives much more impact to the viewer, and in many cases this is the preferred method of information transfer. This paper discusses a particular application in which position, velocity and vehicle diagnostics are collected from race cars in NASCAR races and transformed so that information can be integrated graphically with the video stream from the cameras at the race and presented to the television viewers when appropriate.

Fundamental to the production of graphical information overlays is a set of accurate positions for all the vehicles in the race. In a NASCAR race, there are 43 vehicles, and all of these must be positioned accurately. Accurate relative positions can easily be computed with differential GPS measurements, provided a sufficient number of measurements together giving sufficient geometrical strength are available. Unfortunately, neither of these prerequisites exist at a NASCAR racetrack. So in order to provide continuous and accurate position information, some kind of supplementary measurement is required in addition to GPS. The incorporation of a digital model of the race track into the GPS receiver on every vehicle gives enough additional geometrical strength so that with GPS observations, the accuracy and continuity requirements of the application are satisfied.

Once sufficiently accurate position information for all the cars is generated, this has to be transferred to a central location where it is used to generate positions for the vehicles captured in the various video frames. This is transformed to screen co-ordinates so screen graphics can be generated for those vehicles. These graphics are overlaid onto the video images generated by the cameras at the race.

In order to do all these tasks in real time, sophisticated telemetry, time synchronization and integration subsystems have had to be designed in addition to the custom GPS receiver software used to generate the vehicle positions in first place. This paper will describe the various subsystems and their integration with particular emphasis on the effect of the track model constraints used to aid the GPS positioning. The methodology for integration of the track model constraints into both the pseudo range and Real Time Kinematic (RTK) filters will be described as well as the method used to transform the "real world" vehicle positions into co-ordinates in the video screen frame. Test results will be provided.

INTRODUCTION

The sports entertainment industry's demand for supplementary visual effects has increased over the last 10 years. In auto racing, this comes in the form of position, velocity and vehicle diagnostic information integrated

graphically with the video information supplied by the traditional means, the video camera. An example of this is a system recently developed by Sportvision, PI Research, and NovAtel Inc. for television broadcasts of North American Stock Car Association Races (NASCAR) races. The object of this system is to generate and integrate various types of “real world” position and diagnostic information in the form of graphical annotation with the video stream available to the viewer. The most challenging annotation required is a pointer or other symbol which tracks the motion of the vehicle on the screen. Such annotation requires that four tasks be successfully completed. First of all, accurate “real world” positions for the vehicles in the race must be generated. Second, these have to be transmitted to a central location where the video images can be overlaid. Third, a time relationship between the video images and the “real world” positions must be established and used to generate “real world” positions of the vehicles at the time the video image was formed. Finally, the “real world” 3d position so generated must be transformed to the 2d screen reference frame. Each task is handled by subsystems labelled according to the task they perform as 1) the GPS subsystem, 2) the telemetry subsystem, 3) the time synchronisation subsystem and 4) the video overlay subsystem. This paper will describe more fully what the tasks are and to describe the engineering subsystems used to address them. It will give more detail about the interrelationship between the tasks and how together they can address the total system problem of providing annotated video as a function of the vehicle motion and camera position and setting.

The positioning task had to be capable of providing continuous positions with an accuracy of ½ metre at one sigma. Satellite visibility is obstructed by a steel linked fence next to the race track. The approach taken to solve this problem was to incorporate positionally dependent constraint information based on digital track models to the different GPS filters on the NovAtel Inc. receivers. The methods to do this, and test results showing the accuracy improvements achievable with track model constraints will be described more fully later on.

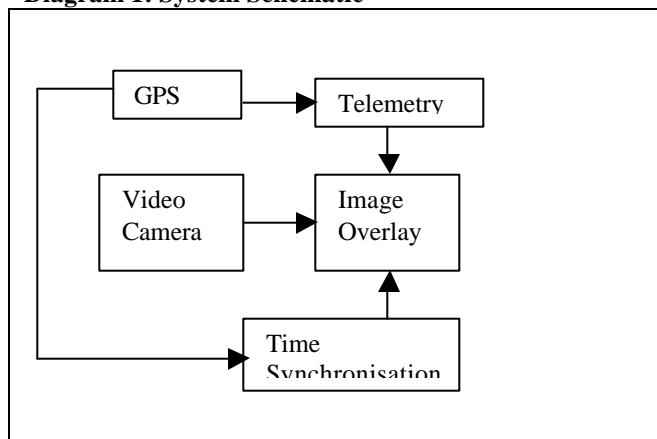
The video overlay task required that real world WGS84 positions be transformed to screen frame co-ordinates. There are up to 6 cameras, 43 racecars, 5 positions per car per second, 30 video images per second and 30 camera settings per second. The method by which the GPS positions of the racecars are transformed to screen co-ordinates will be described.

Although it is not the focus of this paper, it should be noted that the GPS receivers and other hardware used on the race vehicles had to be packaged in an enclosure which could withstand the race vehicle dynamics.

SYSTEM DESCRIPTION

As mentioned previously, this system can be described as having 4 subsystems: 1) the GPS subsystem, 2) the telemetry subsystem, 3) the time synchronisation subsystem and 4) the video overlay subsystem. The GPS subsystem provides GPS positions to the telemetry subsystem and at the same time receives differential corrections from the telemetry subsystem. The GPS positions are time tagged with GPS time. The time synchronisation subsystem provides time synchronisation between the video images and the GPS positions. Based on the derived GPS times of the video images, the video overlay system generates a set of positions for every vehicle in the race and transforms these to screen co-ordinates. A schematic of the system is shown in the following diagram 1:

Diagram 1: System Schematic



Each subsystem has particular problems which must be solved.

The GPS subsystem must provide positions which are accurate to ½ metre at the 1 sigma level so that when these are transformed to the screen, a strong annotation to vehicle association can be made. This is difficult because the grandstand and protective fence around the track restrict the satellite visibility and degrade the signals of the satellites that are available. A GPS alone solution could not provide the accuracy required. Attempts to use other technologies such as low cost inertial and pseudolites and GPS filter modifications such as clock constraints and velocity modelling also fell short of the goal. A new approach using a digital model of the race track gave the necessary accuracy, but this also had its own challenges, for example, once the general mathematical definition of the track model representation was designed, a track model had to be created for each track and somehow loaded onto each receiver. Then the appropriate portion of the track model to be used in the solution had to be determined, and finally the particular model element had to be incorporated into either the pseudorange or RTK

filters. A more complete description of this and associated test results will be given later.

The ephemeris messages are collected at the differential base station receiver and transmitted to the race cars because under racing conditions it is possible for a satellite to be visible for less than the 30 seconds necessary for the racecar receivers to be able to demodulate the entire 50 bits per second ephemeris message broadcast from the satellite.

The telemetry subsystem has the problem of transmitting 5 Hz position data from 43 racecars in real time to a central controller when there are intermittent blockages between some portion of the track and any single location at the track where a receiver could be situated. The way this was addressed was that at each racetrack three or four 900 MHz telemetry receivers were set up so that at least one was visible from every racecar on the track. Then each racecar was assigned a 10 msec time slot in which to transmit a 120 byte message packet holding the last 5 positions of the vehicle and statistical information about the quality of the positions. At the same time it uses the remaining time slots to broadcast differential corrections, system control and an encoded satellite ephemeris message to the 900 MHz telemetry receivers on the racecars.

The time synchronisation subsystem has the problem of time tagging 29.97 Hz video frames with GPS time so that these times can be used to generate interpolated GPS positions of the vehicles on the track. The time synchronisation between GPS positions and video images had to be accurate to 1 millisecond so that at race speed, there was no more than 10 cm error resulting from timing errors. The video frequency oscillator is generated locally and is not synchronous with GPS. A video time stamp is written into the vertical blanking interval (VBI) of every video frame. The vertical sync and associated time stamp are sent to a time synchronisation computer which is also receiving a 1pps signal from a GPS receiver. From this a GPS to video frame offset is computed. At the same time, the positions in the GPS receivers are time stamped with GPS time accurate to 100 nanoseconds. A time association between the time of the GPS positions and the video frames is made. Since the time sources are asynchronous and the GPS is sampled approximately six times slower than the video, the GPS positions are interpolated to generate a GPS position associated with each video frame.

The video overlay subsystem has to transform the WGS84 co-ordinates supplied by the GPS receivers on the racecars into screen co-ordinates and must know the camera position, orientation and field of view even though some of these parameters are changing at a 29.97 Hz rate, and then use these to transform the vehicle

positions at 29.97 Hz. This is a daunting task because as mentioned, there are up to 6 cameras, gathering video images at 29.97 Hz., each of which has its own set of camera parameters used to transform the interpolated 5 Hz position data from real world to screen co-ordinates. Furthermore, the video stream must be delayed between 2.5 and 3 seconds to account for the differential latency in the positions from the GPS subsystem. The transformed positions are used to produce graphical overlays which are merged with the delayed video if and when an operator requests it on his touch screen.

VIDEO OVERLAY DETAILED DESCRIPTION

The work of the video overlay subsystem is performed by a high speed graphical overlay render (GOR) computer. It reads the video and extracts time stamp data from the VBI. This computer also reads the GPS position and time data from the telemetry subsystem. For each video frame, the GOR computer renders a graphic using the interpolated GPS data for the current video frame. In order to do this, it must transform the interpolated position (transformed from WGS84 to state plane co-ordinates) to generate a screen co-ordinate location for the graphical overlay.

The transformation from world (state plane) to screen co-ordinates is described below in two steps. The first step includes a rotation and translation of the world co-ordinates which is based upon the camera location (with respect to the GPS base station) and orientation (with respect to the frame defined by the state plane system in the area). The second step takes a translated and rotated co-ordinate and applies variable scaling depending on the current camera zoom setting.

World co-ordinates are represented as four-dimensional row vectors, so both rotation and translation can be included in the same matrix multiply, and the inverse transformation is then just the matrix invert of the original transformation matrix. The 4X4 transformation matrix from camera co-ordinates to world-co-ordinates can be written as:

$$M_c^w = Rx(\mathbf{p} / 2)Rx(\mathbf{t})Rz(\Theta)T(nx, ny, nz)$$

Where

$$Rz(\mathbf{f}) = \begin{pmatrix} \cos \mathbf{f} & \sin \mathbf{f} & 0 & 0 \\ -\sin \mathbf{f} & \cos \mathbf{f} & 0 & 0 \\ 0 & 0 & 1 & 0 \\ 0 & 0 & 0 & 1 \end{pmatrix}$$

$$Rx(\mathbf{t}) = \begin{pmatrix} 1 & 0 & 0 & 0 \\ 0 & \cos \mathbf{t} & \sin \mathbf{t} & 0 \\ 0 & -\sin \mathbf{t} & \cos \mathbf{t} & 0 \\ 0 & 0 & 0 & 1 \end{pmatrix}$$

$$Ry(\Theta) = \begin{pmatrix} \cos\Theta & 0 & -\sin\Theta & 0 \\ 0 & 1 & 0 & 0 \\ \sin\Theta & 0 & \cos\Theta & 0 \\ 0 & 0 & 0 & 1 \end{pmatrix}$$

$$T(a,b,c) = \begin{pmatrix} 1 & 0 & 0 & 0 \\ 0 & 1 & 0 & 0 \\ 0 & 0 & 1 & 0 \\ a & b & c & 1 \end{pmatrix}$$

$$(nx, ny, nz, 1) = (0, N, 0, 1)Rx(\mathbf{t})Rz(\Theta)T(Cx, Cy, Cz)$$

The world to camera co-ordinates transformation is just the invert of M_c^w defined above

$$M_w^c = (M_c^w)^{-1}$$

$$= T(-nx, -ny, -nz)Rz(-\Theta)Rx(-\mathbf{t})Rx(-\mathbf{p}/2)$$

Then the rotated and translated position is scaled according to the instantaneous camera setting. These parameters include field of view, near and far clipping, aspect ratio and the number of pixels on the screen.

$$P = \begin{pmatrix} \cot(F/2) & 0 & 0 & 0 \\ ar & \cot(F/2) & 0 & 0 \\ 0 & 0 & \frac{-(f+n)}{(f-n)} & -1 \\ 0 & 0 & \frac{-2fn}{(f-n)} & 0 \end{pmatrix}$$

$$xMat = M_w^c P$$

If $(x_0, y_0, z_0, 1)$ represents a point in world co-ordinates,

$$(x_0, y_0, z_0, 1)xMat = (x_1, y_1, z_1, w_1)$$

Then the screen co-ordinates can be written as:

$$x_s = \frac{x_1}{w_1} \quad \text{then} \quad x_p = 0.5x_s p_x + O_x$$

$$y_s = \frac{y_1}{w_1} \quad \text{then} \quad y_p = 0.5y_s p_y + O_y$$

The parameters used are described in the following table, and in more detail after.

Table 1: Broadcast Camera Parameters

Parameter	Description
C_x, C_y, C_z	Camera location
τ	Tilt of camera. $\tau = 0$ when the optical axis is perpendicular with the pan axis
Θ	Pan of camera. $\Theta = 0$ when the optical axis is in the y, z plane.
N	Distance from the pan axis to the camera nodal point.
F	Camera field of view
O_x, O_y	Optical center of the camera lens in pixels
p_x, p_y	Number of pixels in x and y
x_p, y_p	x, y screen coordinate in pixels
ar	Aspect ratio of the image plane
f	Far clipping plane distance
n	Near clipping plane distance

Each broadcast camera has sensors to measure the pan, tilt, and zoom once per video frame. These sensors accurately measure where the camera is pointed and the field of view of the lens and camera combination. The camera tripod is levelled such that the pan axis is vertical with respect to gravity. Camera locations are measured and the sensors are calibrated such that a three space camera model is computed.

The offset between the GPS base station and the optical centre of the camera lens (C_x, C_y, C_z) are measured with the GPS system by placing the GPS antenna on top of the camera and subtracting the offset between the top of the camera and the optical axis of the lens. The lens manufacturer provides a table that specifies the distance between the front of the lens and the optical nodal point as a function of zoom. The optical nodal point represents the origin of the camera co-ordinate system.

The field of view is the angle whose vertex is the nodal point and that intersects the vertical boundary of the image plane and the optical axis of the lens. Field of view is computed by measuring the zoom servo voltage in the camera lens and using a lookup table to map voltage to angle. The pan, tilt, and zoom data is measured synchronously with each video frame 29.97 times per second, once per video frame.

Once the camera location, field of view, pan, and tilt is known, any world co-ordinate can be projected both to the camera and to the video screen co-ordinate space.

GPS SUBSYSTEM DETAILED DESCRIPTION

The core of the GPS subsystem is a set of modified NovAtel Inc. OEM4 GPS receivers. The standard version of the OEM4 is an L1/L2 12 channel receiver capable of either producing or using differential measurements in

both pseudorange and RTK modes. The receivers were modified to incorporate an ephemeris differential message, and to apply track model constraints in the pseudorange and RTK filters.

A track model constraint is a position observation in which only one component of the position is known. On a racetrack, the constraint is perpendicular to the track surface and so as the racecar moves around the track, the direction of the constraint changes. These changes can be represented as a set of continuous planar sections. Each planar section is represented as a triangle. On a typical racetrack the entire track can be modelled accurately by 3000 triangles or less with each triangle being between 5 and 10 metres on a side. The triangles are generated from low flight (300 metres) photogrammetric data and have a vertical accuracy of 10 cm. Each NASCAR track has such a model, and prior to a race, all the OEM4 receivers on the cars are loaded with the digital model for the particular track of the race.

Once the model is loaded onto the OEM4 receiver, the receiver does a search based on its position to find the particular triangle to use as a constraint, and then uses this in either the least squares pseudorange filter or in the Kalman RTK filter. The search is a two dimensional search, with the two dimensional plane being a tangent to a local reference point. To facilitate this, and to minimise the CPU requirements at run time, at power up the loaded track model triangle points are transformed from the geographic frame to the ECEF frame and to the tangent plane used in the search. In addition, every triangle is used to generate a covariance and a weight matrix in the ECEF frame (the frame used for positional computations in the OEM4). Then at run time, the best available GPS position is translated and rotated to the local tangent plane and a search is done to find the appropriate triangle with this position. If the triangle related to that position is found, it is applied in the filter which initiated the search.

In the least squares filter, the filter's approximate position with its associated weight matrix is taken from the triangle in the model. The triangles approximate position is just the mean of the three triangle points offset by the magnitude of the antenna height in a direction normal to the plane formed by the triangle. In the RTK Kalman filter, the triangle position and associated covariance matrix are used as a position update.

The least squares filter generates corrections to the system's ECEF position and clock according to the equation:

$$\delta X = (A^T P A + P_x)^{-1} A^T P \omega$$

Where

δX = correction vector to position vector and clock $[X, Y, Z, Clk]^T$

A = design matrix (nx4) based on satellite to receiver geometry

$$\text{In detail } A = [A_1, A_2, A_3, \dots, A_n]^T$$

$$\text{And } A_i = [\partial R^i / \partial X, \partial R^i / \partial Y, \partial R^i / \partial Z, 1]$$

$$\text{With } R^i = ((X^i - X)^2 + (Y^i - Y)^2 + (Z^i - Z)^2)^{1/2}$$

X, Y, Z = ECEF user position

Xⁱ, Yⁱ, Zⁱ = ECEF satellite position

P_x = Parameter weight matrix (4x4) based on knowledge of the parameters (ie track model position) included in the estimation process.

P = Pseudo range observation weight matrix (nxn) which is diagonal with the diagonal entries being the reciprocal of the variances of the pseudo ranges.

ω = The vector of misclosures between the theoretical observations and the actual observations (pseudo ranges).

The theoretical observations are computed from the positions of the current satellite set and the approximate position defined as the mean position of the vertices of the triangle used.

So

$$\omega = R_{obs} - R^i - Clk$$

$$= R_{obs} - ((X^i - X)^2 + (Y^i - Y)^2 + (Z^i - Z)^2)^{1/2} - Clk$$

The weight matrix for the approximate position and clock is:

$$P_x = C_x^{-1} = (J^T C_t J)^{-1}$$

Where

C_t = The covariance matrix of the position/clock in the planar section or "triangle" frame.

J = The matrix of derivatives of the transformation used to transform the position and clock parameters from the triangle frame to the ECEF frame.

C_x = The covariance matrix of position/clock in the ECEF frame.

The matrix J is a 4 by 4 matrix with the upper left 3 by 3 submatrix being a matrix that will rotate a vector from the triangle frame to the ECEF frame. The 4th row and column are zero except for a one on the 4th diagonal element. The rotation submatrix is easy to generate by simply representing three basis vectors, describing the triangle frame and a normal to it, in the ECEF frame. The differences of these vectors are parallel to the planar section, and the cross product of two of these difference vectors provides a normal vector to the triangle. The cross product of the normal vector with either of the vector differences generates a vector parallel to the triangle and orthogonal to the other two vectors used in the cross product. Finally, normalising these three vectors provides a set of orthonormal basis vectors representing the triangle frame in ECEF co-ordinates. So this set of vectors can be concatenated to generate the rotation submatrix of J, J_R . Symbolically:

$$J_R = [B_1 | B_2 | B_3]$$

Where B_1, B_2, B_3 are the basis vectors whose construction is defined in the previous paragraph. And finally

$$J = \begin{bmatrix} J_R & 0 \\ 0 & 1 \end{bmatrix}$$

The constraint position is given by the average of the three corner positions in the ECEF frame plus the constraint position relative to the planar section, transformed to the ECEF frame. Symbolically, this is:

$$\text{Constraint pos'n: } P_{cp} = ((P_1 + P_2 + P_3)/3.0) + J_R * [0,0,h_a]$$

Where P_1, P_2, P_3 are the ECEF positions of the planar section corners, and h_a is the antenna height with respect to a level planar section.

RT20/RTK FILTER MODIFICATION

The RTK filter in the OEM4 [2] supplements the pseudorange and carrier observations used in the filter with a track model derived position observation. The constraint is actually applied in the floating ambiguity estimation portion (called RT20 [1]) of the RTK filter. This is a Kalman filter that generates estimates of the relative position between a reference and rover receiver as well as estimates of floating ambiguities related to the double difference carrier observations for those two receivers. In the NovAtel Inc. receiver, RT20 provides a best available solution when RTK is not available as well as providing an initial search space for the RTK (fixed integer ambiguity) carrier based process [2].

There are two things that have to be done to resolve ambiguities:

- 1: Guess at an initial position, and an associated search space whose size is based on the precision of the initial position estimate.
- 2: Use the guess and its precision to define a series of candidate sets of ambiguities and then accumulate computed residuals over time and eliminate sets whose residual accumulation exceeds some kind of threshold.

Typically a Kalman filter with both position and ambiguity states is used to define an initial guess for the search space. The Kalman filter used to estimate position and floating ambiguity states can be described as follows:

$$\text{State: } X = [x, y, z, N_1, N_2, \dots, N_k]$$

State Initial Covariance: $P =$ [big diagonal elements, 0 off diagonal elements]

The design matrix H defines the linear relationship between the double difference observation (satellites r_j and the two receivers) and the state elements.

For satellite j and reference satellite r the phase relationship is

$$H = [\Delta x_m^r / R_{r_m}^r - \Delta x_m^j / R_{j_m}^j, \Delta y_m^r / R_{r_m}^r - \Delta y_m^j / R_{j_m}^j, \Delta z_m^r / R_{r_m}^r - \Delta z_m^j / R_{j_m}^j, 0, 0, \dots, 1, 0, \dots, 0]$$

While the pseudo range relationship is

$$H = [\Delta x_m^r / R_{r_m}^r - \Delta x_m^j / R_{j_m}^j, \Delta y_m^r / R_{r_m}^r - \Delta y_m^j / R_{j_m}^j, \Delta z_m^r / R_{r_m}^r - \Delta z_m^j / R_{j_m}^j, 0, 0, \dots, 0, \dots, 0]$$

The Kalman filter mechanization [3] is as follows:

$$\text{Gain: } K_k = P_k (-) H_k^T [H_k P_k (-) H_k^T + R_k]^{-1}$$

$$\text{Covariance Update: } P_k (+) = [I - K_k H_k] P_k (-)$$

$$\text{State Update: } X_k (+) = X_k (-) + K_k [Z_k - H_k X_k]$$

Where

R = Observation covariance matrix (scalar for phase and pseudo range observations), 3 by 3 matrix for position.

z = Observation (pseudo range, carrier or position measurement)

Given the position observation from the track model, the observation to state relationship is very simple

$$H = \begin{bmatrix} 1, 0, 0, 0, \dots, 0 \\ 0, 1, 0, 0, \dots, 0 \\ 0, 0, 1, 0, \dots, 0 \end{bmatrix}$$

$H = [I, 0]$ with $I = 3 \times 3$ and $0 = 3 \times (n-3)$, (n = number of states)

And $R = C_x$, the covariance matrix of the constraint position:

$$C_x = J^T C_t J$$

Where

C_t = The covariance matrix of the position in the "triangle" frame.

J = The matrix of derivatives of the transformation of position from the "triangle" frame to the ECEF frame. In this case J is just a 3 by 3 rotation matrix.

$$C_t = \begin{bmatrix} 10000, & 0, & 0 \\ 0, & 10000, & 0 \\ 0, & 0, & 0.01 \end{bmatrix}$$

that is, the parallel elements are more or less unknown, and the normal element is known to 10 cm at 1 sigma.

The advantage of including position constraints with the GPS observation set is that the precision of the initial position estimate used to define the search space can be reduced sooner and more.

TEST RESULTS

The results shown here are based on data collected during two tests at the Fontana race track (California speedway) in Ontario, California. The first set of results was generated in post mission from data collected in

September 2000. The second set was generated during a real time test that took place in February 2001.

Modifications were made to the least squares filter first, and even operating in single point mode gave dramatically improved results, and this served as a motivator to implement the RTK modifications. The offline RTK results are more germane, so these are described. The Fontana data collected last September are used to generate constrained and unconstrained position results. The items of particular interest were resolution reliability and the time to resolution possible when constraints are available compared to when they are not. The improvement in resolution time can be seen by forcing the ambiguity filters (both RT20 and RT2) to reset 10 seconds after every resolution, and then allowed the ambiguities to be re-resolved. The accuracy of the system can be verified by the results generated with continuous RTK positions because the test car was driven on a portion of the track where the satellite coverage was good (more than 6 satellites).

TABLE 2: Post Mission RT20 Performance Statistics

Case	Unconstrained	Constrained
Number Samples	628	146
Horizontal RMS	0.35 m	0.55 m
Horizontal Max	0.94 m	1.74 m
Vertical RMS	0.46 m	0.16 m
Vertical Max	2.03 m	0.33 m
Number Resolutions	19	41
Resolution Time	51 sec	24 sec
Duration	972 sec	972 sec

A comparison of the results of the constrained and unconstrained cases with the continuous RTK case showed that all the resolutions were correct.

Since the track model is primarily a height constraint, the vertical errors in the constrained case are much smaller. The large horizontal maximum error in the constrained case is a result of poor geometry, and the standard deviations of the position at this time reflects this. If the unconstrained system had dealt with the same geometry in the same mode, then its error would have been high there too. The reason the RT20 RMS is higher for the constrained case is because so much more of the positions computed are in the high variance portion of the floating ambiguity convergence curve. So the RMS appears worse because the constrained system spends less time in RT20 and more time in RT2 mode. Note that the unconstrained case has more samples in RT20 mode because it took much longer to resolve ambiguities.

Based on the preliminary offline results, modifications were made to the real time OEM4 software in order to test the process in real time.

FONTANA FIELD TRIALS FEB 13,14,15, 2001

On Feb 12, 2001, a NovAtel Inc. team met in Ontario, California, the site of the California Speedway (Fontana racetrack) for a race track trial. The object of the trial was to validate the modifications made to the OEM4 software in a real time test. For successful validation, 4 criteria had to be met:

1. The receiver must have no serious system level degradations, including memory errors or significant CPU overloads.
2. The accuracy of the constrained system had to be better than that of the unconstrained system.
3. The resolution time of the constrained system had to be less than that of the unconstrained system.
4. The reliability of the constrained system had to be better than that of the unconstrained system. In other words, there had to be fewer incorrect resolutions.

In order to do this, a comparison of the results from a modified OEM4 was made with the results from a standard OEM4 configured as an RTK receiver. The two receivers processed signals received from a single antenna mounted on the roof. The base station telemetry line was split so both receivers had access to identical RTCA range and phase observations.

The Fontana track is an oval track approximately 3.5 km long, with banks of about 20 degrees on the east and west ends. A 40 metre high grandstand extends the length of the south side of the track and provides decent obstruction to the receivers of satellites in the southern sky when the receivers are on the south side of the track. Between the track and the grandstand is a wire mesh fence designed to catch debris that results from normal and abnormal race conditions. The fence is 7 metres high and extends about 3 metres over the edge of the track. It consists of 15 cm square wire mesh and generates significant perturbations in the GPS signals.

The track itself is 16.8 metres wide and is divided into five 3.4 metre wide lanes. For the purposes of test control we tried as much as possible to follow the divisions between the pavement lanes. Then height comparisons from one lap to the next can be made and good agreement should indicate the system is working better than if the lap to lap comparison is not good. There were 4 divisions or rows, which are labeled Row 1 to Row 4. Row 1 is next to the infield, and is relatively unobstructed. Row 4 is adjacent to the fence (3.4 metres away), and with the fence overhang, exactly 1/2 of the sky is at least partially obstructed. Row 1 can be seen under the car in the following picture.

Picture 1 Fontana Racetrack, Tom, rental car and “Row 1” under center of car



TEST DEFINITION

The test itself took place over 2 days, Feb 14 and 15. On the first day each of the “rows” were driven 3 times without any artificial resets. The objective on the first day was to overcome some installation difficulties and ensure that the system worked.

TEST RESULTS FEB 14

The Feb 14 results show fairly consistent results between the data collected on Rows 1, 2 and 3 but significant discrepancies in Row 4. But even on Row 1 where the coverage was relatively good, during an early RTK reset, the height standard deviation reached just 0.25 metres on the constrained model, compared to 1.7 metres for the standard OEM4, and the resolution time was 50 seconds compared to 90 seconds for the standard OEM4.

Row 4 results from day 1 showed the constrained system has resolved ambiguities almost continuously, but the standard system never reaches a fixed ambiguity state. For the last three laps of the row 4 experiment we drove on the track between row 4 and the track wall, in what was the most obscured portion of the track. In this location we stopped and allowed the systems to resolve three times (not always at the same point on the track). During each of these resolutions, the standard OEM4 resolved improperly and the track model OEM4 resolved correctly as was verified by comparisons with control later on in the real time test. This shows that the constrained OEM4 receiver is, in this particular case, more reliable than the standard OEM4.

The height vs time plots (figure 1 and 2) below show the repeatability improvement of the constrained over the standard OEM4. The secondary axis of both plots show the height standard deviation. The standard deviation of the standard model is rarely below 1 metre in the standard OEM4 case and rarely above 0.25 metres for the constrained OEM4 case.

Figure 1: Fontana Feb 14 Standard OEM4 Row 4 Height and Height Stdev vs Time

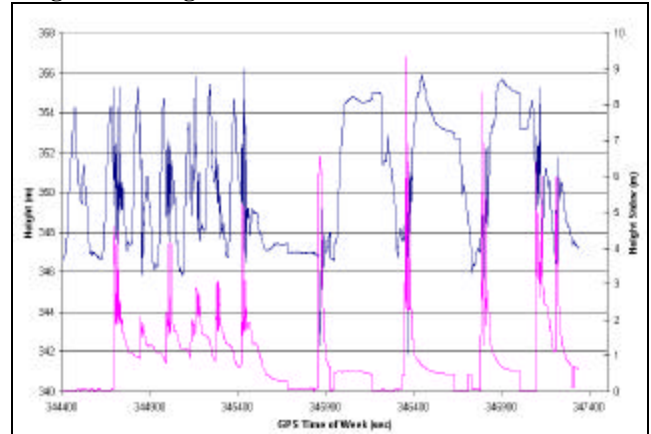
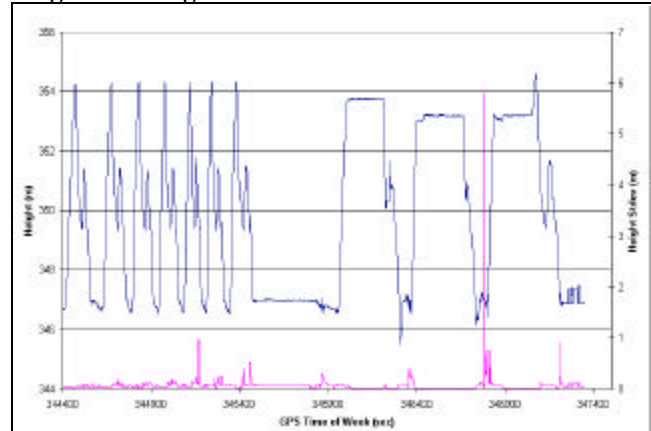


Figure 2: Fontana Feb 14 Track Model OEM4 Row 4 Height and Height Stdev vs Time



On day 1, the number of satellites was about the same (between 4 and 6) for both receivers, and the idle time, which is a reflection of the CPU load, was between 50 and 60 percent. This, plus the consistency of the results from the constrained system, indicates that there is no significant system level degradation as a result of the track model constraint logic.

TEST RESULTS FEB 15

The objectives of the experiment on this day were to determine the difference in resolution times between the two systems, to obtain accuracy estimates for the real time positions and to find out if the constrained system was resolving properly. The testing methodology on Feb. 15 was similar to that of the Feb 14 tests. We used each of the 4 pavement divisions at a driving guide in order to generate a repeatable path to follow on increasingly obstructed areas of the racetrack. Row 1 is the least obstructed.

Each row was driven 11 times with the standard OEM4 and track model OEM4 combination. On rows 1 and 2,

filter reset commands were issued to the filter to re-initialize the carrier measurement ambiguities. The object of this was to measure the difference in ambiguity resolution times for the 2 receivers when the constellation was good. Since the first two rows were relatively unobstructed, the position errors of both systems could be computed from post mission RTK results. Using these and the reported standard deviations from both systems, a ratio of position error divided by reported standard deviation could be made. Then, when the obstructions made comparisons with RTK positions impossible, a level of system error could be hypothesised from the reported standard deviations. For rows 3 and 4 it was not necessary to issue reset commands because signal blockages in those rows caused the filter to reset anyway. On these rows, the reported standard deviations and the position repeatability is the only indication of the system reliability.

The figures 3 and 4 show row 1 results that indicate the effect of continuous RT2 resets on the two systems (standard system on top, height vs time on the left, height vs longitude on the right). Note that the scale for the height on the right hand axis of figure 3 is twice that of the horizontal scale on the left. In real time both receivers were allowed to resolve ambiguities, and then a reset command was issued. The resolution time in both receivers was not the same, so the commands were issued asynchronously. The commands were issued at different places in the track so the effect of different constellation shadowing could be observed. The effect of the reset command is to force the the receiver to discard all of the RTK ambiguity information (for both the float and fixed ambiguity filters) and return to pseudo range differential mode. The height repeatability is much better on the track model heights, and the resolution time is much less. The height standard deviation for the standard model in unresolved mode is between 2.5 and 0.7 metres, while the constrained height standard deviation varies between 0.25 and 0.1 metre in unresolved mode. The average resolution times for the standard and constrained system are 3 minutes and 25 seconds respectively. There were between 4 and 7 satellites tracked on both receivers.

The following figures 3 and 4 show the difference between the real time positions with their reset induced errors and completely (and correctly) resolved positions generated without resets in post mission. The heights on the constrained OEM4 are more consistent than the heights for the standard OEM4, but the plots indicate that when the system is not resolved, the maximum horizontal error level is not too different for the two systems. However in the track model case the time the system stays in non-fixed ambiguity mode is much less, so the duration of the time when the constrained system has large errors is much less. Also, the component with the

highest error (by a factor of two), namely height, has been reduced significantly.

Figure 3: Fontana Feb 15 Standard OEM4 Row 1 Position Error vs Time

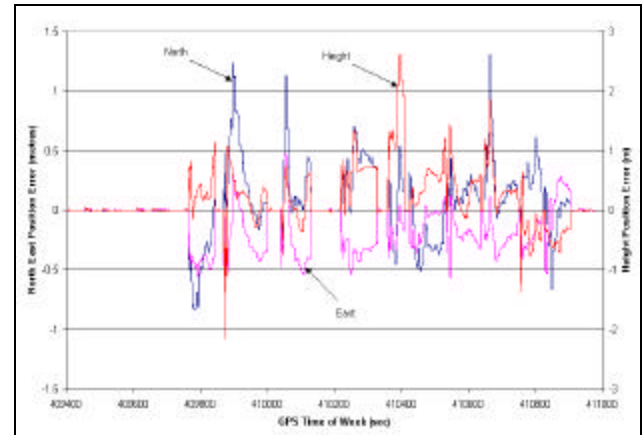
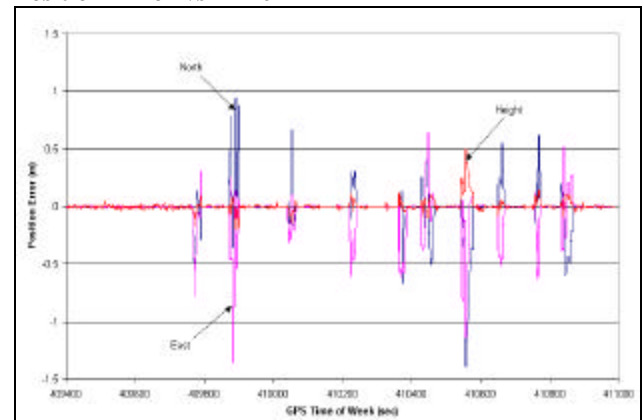


Figure 4: Fontana Feb 15 Track Model OEM4 Row 1 Position Error vs Time



The following figures 5 and 6 show the standard deviations for the standard OEM4 and constrained OEM4 respectively.

Figure 5: Fontana Feb 15 Standard OEM4 Row 1 Standard Deviation with Resets (Height Stdev is red)

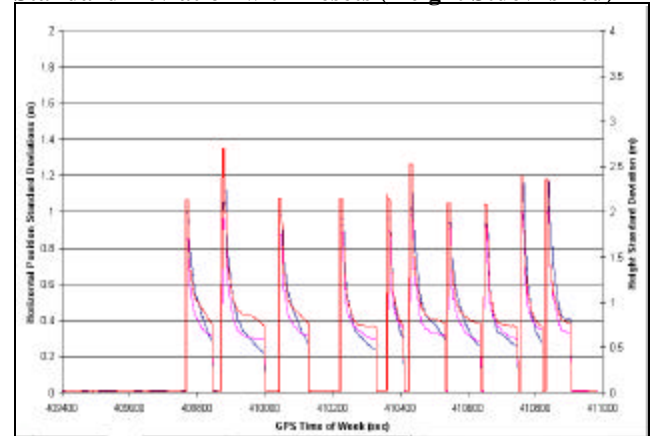
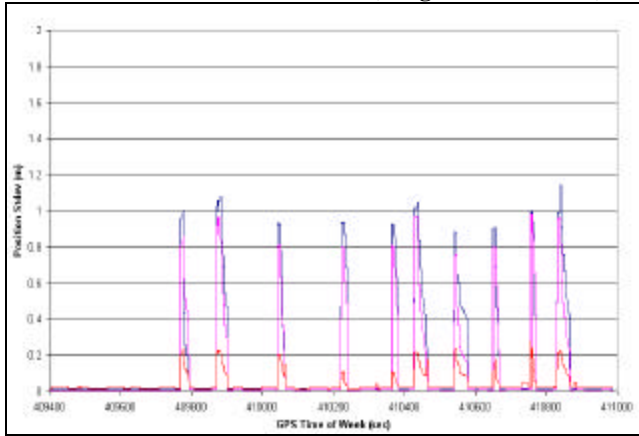


Figure 6: Fontana Feb 15 Track Model OEM4 Row 1 Standard Deviation with Resets (Height Stdev is red)



For every epoch of the data set related to the above test in which the system did not have fixed ambiguities, the ratio of the each axis error to its associated standard deviation was computed (ie error seen in Fig 3 divided by standard deviation seen in Fig 5). Then the means of all these ratios for every axis and both systems were generated. These mean ratios are summarized below:

Table 3: Mean Ratio Axis Error and Standard Dev

System	North	East	Height
Standard	0.66	0.64	0.52
Track Model	0.58	0.68	0.74

This indicates that the standard deviations are a conservative representation of the actual errors in both systems. The row 3 and 4 data for the standard OEM4 case are more erratic than they were in the row 1 and 2 tests. Row 3 is 6.6 metres away from the overhanging fence, and so there were enough natural obstacles so the systems normally had RTK resets at least once per lap. In the standard OEM4, the heights are clearly more erratic. The standard deviations for that version indicate height errors that vary between 1 and 7 metres. The standard version managed 4 fixed ambiguity resolutions, and the constrained version was able to resolve 18 times. Since the graphical results for row 3 are somewhat similar to the row 4 results, only the row 4 results will be shown.

The following figures 7 and 8 generated from row 4 data show the increased variability of height over time for the standard OEM4 compared to the constrained OEM4. The standard deviations of the heights are usually 2 metres or more for the standard OEM4 but usually less than 0.25 metres for the constrained OEM4.

Figure 7: Fontana Feb 15 Row 4 Standard OEM4 Height, Height Standard Deviation vs Time

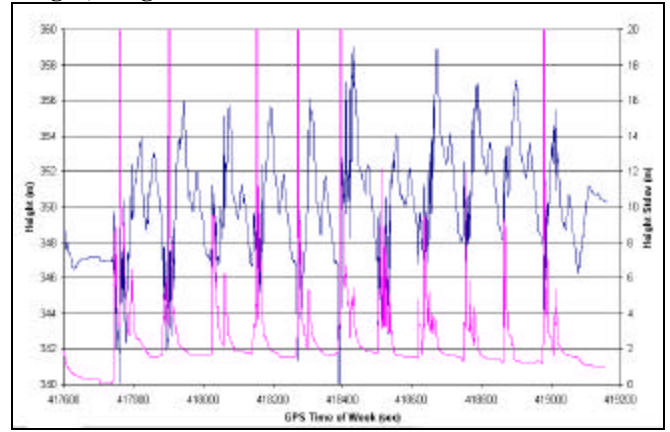
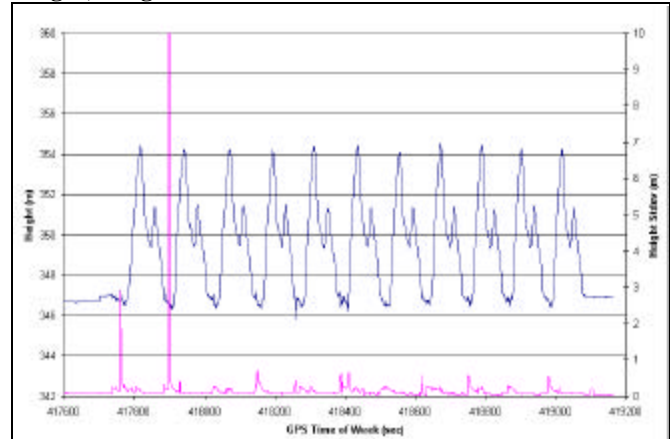


Figure 8: Fontana Feb 15 Row 4 Track Model OEM4 Height, Height Standard Deviation vs Time



The figures 9 and 10 below show qualitatively the improvement of the constrained OEM4 over the standard OEM4. These show the height vs longitude for the row 4 trajectory. The noise level on the standard OEM4 is more than the total difference in height in the north south direction. The constrained OEM4 shows repeatability within 0.5 metres except for one excursion which occurred because the horizontal position used to search for a track model triangle was computed with poor geometry and was outside the boundaries of all the triangles of the track model, so no constraint could be found for it. The standard deviation of the height at this point is about 300 metres for both systems. This type of error has since been eliminated simply by extending the planar section boundaries past the edge of the pavement.

Figure 9: Fontana Feb 15 Row 4 Standard OEM4 (Height vs Longitude)

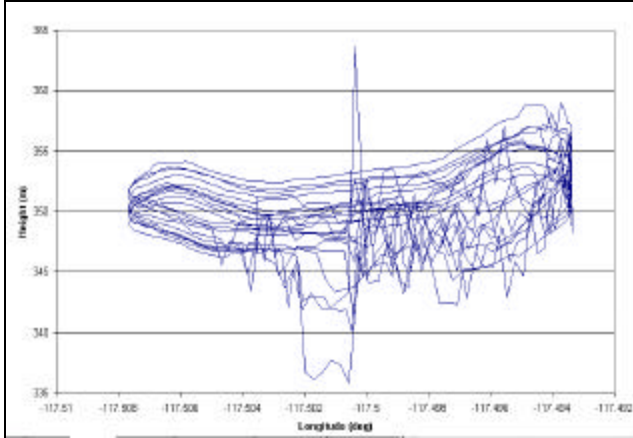
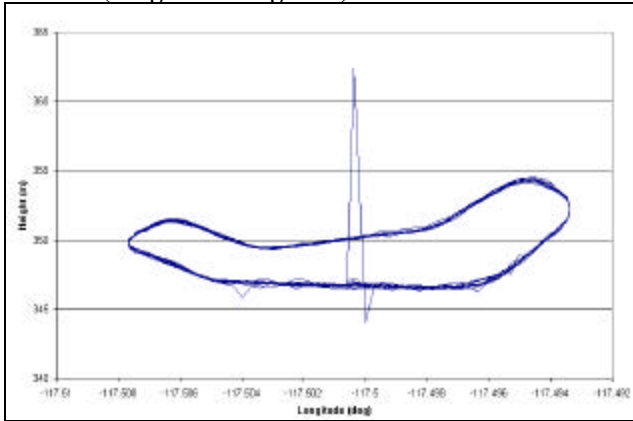


Figure 10: Fontana Feb 15 Row 4 Track Model OEM4 (Height vs Longitude)



The magnitude of the horizontal errors can be estimated by the size of the standard deviations reported by the two systems. Furthermore, in the portions of the test that did not incorporate operator induced resets, some estimate of the expected operational accuracy can be made. This is based on the computed standard deviations and the assumption that the standard deviations computed actually do represent the errors in the system. This assumption is a reasonable one given the results of the controlled reset test carried out on the data from row 1 collected Feb 15 in which the standard deviations are a fair reflection of the measured error levels on both the standard OEM4 and track model OEM4 systems (see Table 3). In order to quantify the error level of single axis positions, all the single axis standard deviations were put into 0.0 m to 0.5 m, 0.5 m to 1.0 m and greater than 1.0 m categories. The total for each category was generated. Since data was collected from different rows for different lengths of times, the accumulations are normalised as if each row collected 1000 seconds of data. The computed percentage of points in each category for both receiver types are shown in the following table 4. If a set of positions is to satisfy the requirement that it meets the 0.5 metre error level at 1 sigma, then 68% of its position

errors should be less than 0.5 metres. Similarly, the 2 sigma 1 metre requirement will be met if no more than 5% of the position errors exceed 1.0 metres.

Table 4: Summary Reported Error Distribution

Model Axis	Require Less than 32% > 0.5 for 68%	Require Less than 5% >1.0 for 95%
Std N	20.1 (pass)	9.1 (Fails)
Std E	19.3 (pass)	9.1 (Fails)
Std U	36.9 (Fails)	34.5 (Fails)
TM N	11.6 (pass)	5.1 (close enough)
TM E	10.3 (pass)	3.2 (pass)
TM U	0.6 (pass)	0.1 (pass)

The results show that the standard model fails to meet the requirements of 1.0 m 95% of the time and at 0.5 m 68% of the time. The OEM4 with supplementary track model constraints has no difficulty with the 68% 0.5 m requirement and is within acceptable limits for the 95% 1.0 m requirement.

When the track model constraints act on the constrained system, the horizontal standard deviations are almost always less than 3 metres, while the standard OEM4 has standard deviations which reach over 50 metres. Therefore, the track model is a significant help with the horizontal positions when the geometry is poor. This is partly because knowledge of height makes the other components more observable, but also because the tilt of the planar sections makes a portion of the horizontal position directly observable via the constraint. This is interesting because as the vehicle moves around the track composed of inwardly pointing planar sections, all of the position components are at one time or another directly observable by the planar section constraints. Provided the system can maintain carrier tracking on a minimal number of satellites, the accuracy improvement provided at one portion of the track can be carried forward to another portion of the track over which a different position component becomes observable. In this way eventually (say after 1/4 lap), all the position components can become known. Simulation shows that if a 10 cm position observation is applied as a height constraint in an ambiguity estimation system, the resulting height will have a standard deviation of 10 cm. Then if the constraint direction tilts away from the zenith towards one of the horizontal position components, then that component is reduced according to the magnitude of the tilt angle. This is shown in table 7:

Table 7: Horizontal Effect

Tilt Angle (deg)	Horizontal Component Std Dev
5	1.4 m
10	0.8 m
20	0.40 m
40	0.20 m

GRAPHIC EXAMPLE

So as not to forget the reason for going to the effort of designing the system described in this paper, an example of the type of race graphic is included.



CONCLUSIONS

A system which provides real time graphical annotation based on racecar positions has been described. There are four major components to such a system, namely telemetry, time synchronization, GPS positioning and video overlay components.

Detailed descriptions of the video overlay system including the transformation used to convert a position from the geographic frame to the video screen frame has been included.

A detailed description of the methodology used to incorporate a track model into either a GPS pseudorange least squares position filter or a GPS pseudorange/carrier Kalman position/ambiguity filter has been given.

The track model constraints make it possible for the system to provide 1.0 m accuracy in all axis at the 2 sigma level (95%) or 0.5 m accuracy at the 1 sigma (68%) level in a restricted environment such as the Fontana racetrack. From the test it is evident that the track model constraints improve the positioning accuracy significantly, up to a factor of 10 in many cases and sometimes more. In most cases, the improvement is in height as one would expect, but in conditions of poor geometry the horizontal accuracy is also much better (sometimes more than 100 times better) in the constrained case.

The horizontal accuracy also improves depending on the slope of the constraining section with respect to the local level because if there is a significant slope, then a component of the planar section's normal vector will be parallel to the local level plane. The horizontal accuracy improves as a function of the variation (that occurs with

position change as the vehicle moves down the track) in the slope of the triangle section.

The track model implementation on the OEM4 receiver is correct. There were a total of 11400 seconds of data, and less than 10 with height position errors of 1 metre or more.

The reported standard deviations on the track model enhanced OEM4 accurately reflect the position errors in the system.

The track model OEM4 never generated a noticeably incorrect ambiguity resolution, even when the standard OEM4 receiver did (3 occurrences of this).

The total system provides the type of annotation required to enhance the television production.

ACKNOWLEDGEMENTS

The authors would like to thank the following people for their contributions to the project: Mike Bobyne, Ian Williamson, Kim Deimert, Jason Hamilton, Jason Jones, Pat Fenton of NovAtel Inc., Roberto Peon, Andrew Robbins, Jim McGuffin, Marv White, and Stan Honey of Sportvision Inc., Michael Brown and Steve Lieber of Steve Lieber and Associates. Thanks to Janet Neumann for her review of the paper.

REFERENCES

- [1] Ford, T.J. and J. Neumann, NovAtel's RT20 - "A Real Time Floating Ambiguity Positioning System", Proceedings of ION GPS '94, Salt Lake City, Utah, Sept. 20-23, 1994, The Institute of Navigation, Washington, D.C. pp. 1067.
- [2] J. Neumann, A. Manz, T. Ford, O. Mulyk, "Test Results from a New 2 cm Real Time Kinematic GPS Positioning System", Proceedings of ION GPS '96, Kansas City, Mo., Sept. 17-20, 1996, The Institute of Navigation, Washington, D.C. pp. 183
- [3] R.G. Brown, P.Y.C Hwang, **Introduction to Random Signals and Applied Kalman Filtering** 3rd edition, John Wiley and Sons, 1997
- [4] T. Ford, K. Milnes, "Track Model Constraint Enhancement for NovAtel's OEM4", presented at Kinematic Systems Conference (KIS), Banff, Alberta, June 2001.